

least 2/7 that of any nucleus present, a reaction diameter is difficult to imagine. Thus, the typical Butler diffraction patterns are probably not well defined in the angular distribution of the continuing fragment even at higher bombarding energies where plane waves are more nearly applicable. Much more work with various bombarding energies is needed to fill out these tentative suggestions or to discard them for a better understanding of the reaction mechanisms.

A cluster interpretation of nuclear transformations involving lithium projectiles has been previously sug-

gested by Bashkin,<sup>22</sup> although in somewhat more detail than ours.

#### ACKNOWLEDGMENTS

This work was part of a program of research under the sponsorship of Professor S. K. Allison. We are indebted to him for aid in the preparation of this paper. We wish to thank Larry Palmer and John Erwood for operation and maintenance of the Van de Graaff accelerator and the electronic equipment.

<sup>22</sup>S. Bashkin, University of Iowa Report SUI-61-6 (unpublished).

## Nuclear Reactions Induced by the Nitrogen Bombardment of Boron-11, Fluorine, Aluminum, Silicon, Phosphorus, and Chlorine

E. NEWMAN AND K. S. TOTH

*Oak Ridge National Laboratory, Oak Ridge, Tennessee\**

(Received 24 August 1962)

Cross sections as a function of bombarding energy were obtained from thick target yields for twelve reactions induced by 27.5-MeV nitrogen ions accelerated in the ONRL 63-in. Cyclotron. Materials containing the following six elements were bombarded: boron, fluorine, aluminum, silicon, phosphorus, and chlorine. The irradiated materials were  $\gamma$  counted and the radioactive products were identified by their characteristic  $\gamma$  rays and half-lives. The following nuclides were observed: Ne<sup>23</sup> from B<sup>11</sup>; P<sup>30</sup> from F<sup>19</sup>; K<sup>38</sup> from Al<sup>27</sup>; Cl<sup>34m</sup> and K<sup>38</sup> from silicon; Sc<sup>43</sup> from P<sup>31</sup>; Sc<sup>43</sup>, Sc<sup>44</sup>, Sc<sup>44m</sup>, Ti<sup>45</sup>, and V<sup>47</sup> from Cl<sup>35</sup>; and Cr<sup>49</sup> from Cl<sup>37</sup>. The observed cross sections are in general agreement with those obtained from other heavy-ion induced reactions at these energies. For the target nucleus Cl<sup>35</sup> it was possible to identify five products, and experimental cross-section ratios were compared to the theoretical ratios determined from Monte Carlo evaporation calculations.

#### INTRODUCTION

ONE of the many reaction mechanisms available for study with incident heavy ions is the formation and subsequent decay of a compound system via the evaporation of light particles. Heavy ions are particularly useful in producing a compound system because of the large excitations available at relatively low bombarding velocities. It has been found from previous experiments with N<sup>14</sup> ions at these energies that, with the exception of transfer reactions, direct interactions are essentially negligible.<sup>1</sup> The predictions of the statistical theory of compound nucleus decay should, therefore, be directly applicable to the distribution of final nuclei after the decay of the compound system.

Several workers have previously determined total cross sections for compound nucleus reactions induced by 27.5-MeV N<sup>14</sup> ions. Targets which have been studied include carbon,<sup>2</sup> beryllium,<sup>3</sup> boron and oxygen,<sup>4</sup> alu-

minium,<sup>5</sup> sodium,<sup>6</sup> potassium,<sup>7</sup> and sulfur.<sup>8</sup> In the present work, total cross sections were determined as a function of bombarding energy for twelve reactions leading to radioactive end products. In all, six different target materials were bombarded. Information concerning these reactions is summarized in Table I. The observed final products can be made by various combinations of emitted particles starting with a given compound nucleus. The assumed decay mode for a particular end-product is also listed in the table. The investigated reactions supplement the previous measurements and provide a more complete picture for reactions initiated by the nitrogen bombardment of elements ranging from lithium to potassium.

#### EXPERIMENTAL METHOD

The following materials were irradiated in the 27.5-MeV N<sup>14</sup> deflected beam of the ORNL 63-in. Cyclotron:

<sup>5</sup> W. H. Webb, H. L. Reynolds, and A. Zucker, *Phys. Rev.* **102**, 749 (1956).

<sup>6</sup> M. L. Halbert, T. H. Handley, and A. Zucker, *Phys. Rev.* **104**, 115 (1956).

<sup>7</sup> J. J. Pinajian and M. L. Halbert, *Phys. Rev.* **113**, 589 (1959).

<sup>8</sup> D. E. Fisher, A. Zucker, and A. Gropp, *Phys. Rev.* **113**, 542 (1959).

\* Operated for the U. S. Atomic Energy Commission by the Union Carbide Corporation.

<sup>1</sup> A. Zucker, *Ann. Rev.* **10**, 27 (1960).

<sup>2</sup> H. L. Reynolds and A. Zucker, *Phys. Rev.* **96**, 1615 (1954).

<sup>3</sup> H. L. Reynolds and A. Zucker, *Phys. Rev.* **100**, 226 (1955).

<sup>4</sup> H. L. Reynolds and A. Zucker, *Phys. Rev.* **102**, 237 (1956).

TABLE I. Assumed de-excitation modes and their  $Q$  values.

Target nucleus	Compound nucleus	Observed nucleus	Particles emitted	$Q$ (MeV)
B <sup>11</sup>	Mg <sup>25</sup>	Ne <sup>23</sup>	2p	2.10
F <sup>19</sup>	S <sup>33</sup>	P <sup>30</sup>	p2n	-1.86
			(3n) <sup>a</sup>	-2.64
Al <sup>27</sup>	Ca <sup>41</sup>	K <sup>38</sup>	p2n	-8.98
			(3n) <sup>a</sup>	-9.76
Si <sup>28</sup>	Sc <sup>42</sup>	Cl <sup>34m</sup>	2α	1.02
Si <sup>28</sup>	Sc <sup>42</sup>	K <sup>38</sup>	α	7.73
Si <sup>29</sup>	Sc <sup>43</sup>	K <sup>38</sup>	αn	-0.75
P <sup>31</sup>	Ti <sup>45</sup>	Sc <sup>43</sup>	pn	-0.76
			(2n) <sup>a</sup>	-1.54
Cl <sup>35</sup>	Cr <sup>49</sup>	Sc <sup>43</sup>	αpn	-7.76
			(α2n) <sup>a</sup>	-8.54
Cl <sup>35</sup>	Cr <sup>49</sup>	Sc <sup>44</sup>	αp	1.95
Cl <sup>35</sup>	Cr <sup>49</sup>	Ti <sup>45</sup>	α	10.40
Cl <sup>35</sup>	Cr <sup>49</sup>	V <sup>47</sup>	pn	0.52
			(2n) <sup>a</sup>	-0.27
Cl <sup>37</sup>	Cr <sup>51</sup>	Cr <sup>49</sup>	2n	0.29

<sup>a</sup> Particles emitted to form the parent of the observed nucleus. In each instance noted above, the parent's half-life is short so that the measured yield of the investigated product includes, in addition, the yield of the parent nucleus.

boron enriched in B<sup>11</sup>, rubidium fluoride, aluminum, silicon, red phosphorus, and rubidium chloride. Reactions with rubidium are precluded because the Coulomb barrier presented by that element is much greater than the bombarding energy. The beam energy was determined to be 27.5±0.4 MeV, using the method of Halbert and Zucker.<sup>9</sup> With the exception of aluminum, which was bombarded in the form of a thick metal foil, the materials were pressed into 3/4-in.-diam brass molds with a hydraulic press. Targets prepared in this way had a smooth hard surface and contained sufficient material so that they were thicker than the range of the incident N<sup>14</sup> beam. The targets were bombarded directly in a Faraday cup assembly so that the beam current could be integrated. Nickel absorbers used to lower the bombarding energy could be placed directly in the Faraday cup. In this manner the effective charge of the nitrogen beam after passing through the nickel foils did not have to be considered. Bombardment times varied with the half-life of the particular radioactive product under study.

The investigated reaction products could be unambiguously identified by the combination of their half-lives and  $\gamma$ -ray energies except in the bombardment of chlorine, where the scandium and titanium fractions had to be chemically separated because of the similar half-lives of three of the products: Ti<sup>45</sup>, Sc<sup>44</sup>, and Sc<sup>43</sup>. A further complication is that Ti<sup>45</sup> decays only by positron emission and has no characteristic  $\gamma$  rays. The chemical procedure used to separate the titanium and scandium fractions was the one described earlier by Fisher *et al.*<sup>8</sup> The chemical yields were quite reproducible and averaged about 80% for the titanium fraction and 50% for the scandium.

After bombardment, the materials were carefully

 TABLE II. Identifying  $\gamma$  radiations and their branching ratios.

Isotope	Half-life	$\gamma$ radiation (MeV)	$\gamma$ -ray branching ratio	$\beta$ + branching ratio
Ne <sup>23</sup>	40 sec	0.438	32%	
P <sup>30</sup>	2.5 min	Annihilation radiation		100%
Cl <sup>34m</sup>	32 min	0.145	31%	
K <sup>43</sup>	7.7 min	Annihilation radiation		100%
Sc <sup>43</sup>	3.92 h	0.374	14%	88%
		Annihilation radiation		
Sc <sup>44</sup>	4.0 h	1.16	100%	95%
		Annihilation radiation		
Sc <sup>44m</sup>	2.44 day	0.27	100%	
		1.16	100%	
		Annihilation radiation		95%
Ti <sup>45</sup>	3.1 h	Annihilation radiation		85%
V <sup>47</sup>	31 min	Annihilation radiation		97%
Cr <sup>49</sup>	42 min	0.089	30%	

removed from the molds and deposited in counting cups which were then placed directly on a NaI crystal connected to a 256-channel pulse-height analyzer. The 1 1/2 in. × 1 1/2 in. NaI crystal was calibrated for the particular counting geometry by the use of several  $\gamma$ -ray standards. A relative photopeak efficiency curve was constructed from the known decay characteristics of Sc<sup>46</sup>, Co<sup>58</sup>, Fe<sup>59</sup>, Co<sup>60</sup>, Zn<sup>65</sup>, Y<sup>88</sup>, Cd<sup>115m</sup>, and Sb<sup>125</sup>. In this way the  $\gamma$ -ray energy region from 0.18 to 1.8 MeV was spanned. This curve could then be made absolute by determination of the absolute disintegration rate of one or more of the samples. Three sources, Na<sup>22</sup>, Co<sup>58</sup>, and Zn<sup>65</sup>, were  $\beta$  counted in a shielded Geiger counter with a known counting efficiency to provide this calibration. The error in the absolute photopeak efficiency is estimated to be 15%. For all of the investigated isotopes the absolute  $\gamma$ -ray counting rate was corrected for the  $\gamma$ -ray branching ratio, decay during bombardment, and beam intensity to obtain the absolute yields per incident particle. When chemical separations were performed, the chemical yields were also taken into account. The identifying half-lives, gamma radiations, and the branching ratios that were used to calculate the reaction yields are shown in Table II.

## RESULTS AND DISCUSSION

### General

The yields per incident particle obtained as a function of incident N<sup>14</sup> energy are shown in Figs. 1, 2, and 3. Several reaction products decay with the emission of more than one  $\gamma$  ray. For these reactions the yield was calculated for each  $\gamma$  ray and in all cases agreed to within 6%. The scatter of the experimental points at a given energy indicates the relative error inherent in the

<sup>9</sup> M. L. Halbert and A. Zucker, Phys. Rev. **121**, 236 (1961).

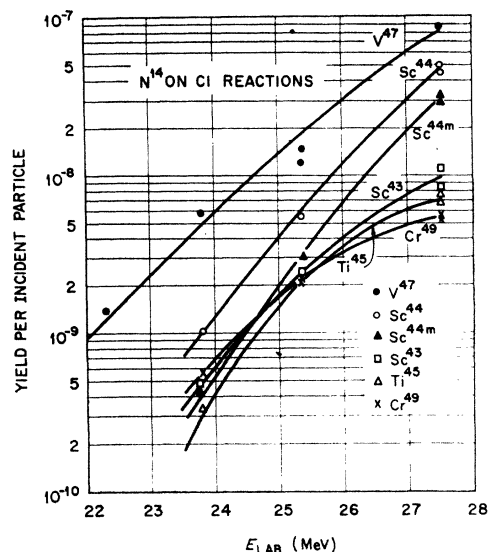


FIG. 1. Yields of radioactive products resulting from  $N^{14}$  on chlorine.

thick target yields. This error arises from uncertainties in beam intensity, counting statistics, and the incident  $N^{14}$  beam energy. Smooth curves were drawn through each set of experimental points. Cross sections as a function of bombarding energy were then determined by differentiating these smooth curves. For this determination the stopping power of each target material for  $N^{14}$  ions was required. The stopping powers were calculated in a manner previously described.<sup>5,6</sup> The probable error in the absolute cross sections is estimated to be about 30%, taking into account uncertainties in crystal calibration,  $\gamma$ -ray branching ratios, slope of the yield curve, and in the stopping power. The excitation functions are shown in Figs. 4 and 5. For those reactions that were studied at just two bombarding energies, the cross sections were calculated only for the midpoint energy. These cross sections are listed in Table III.

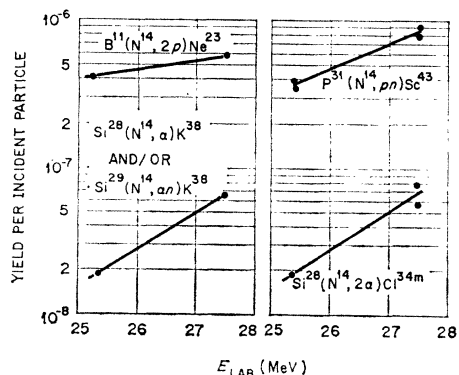


FIG. 2. Yields from reactions induced by  $N^{14}$  ions on phosphorus, silicon, and boron-11.

## Chlorine

The bombardment of natural abundance chlorine ( $Cl^{35}$ , 75.53%;  $Cl^{37}$ , 24.47%) resulted in the identification of six radioactive products. Experimental yields are shown in Fig. 1, and excitation functions are displayed in Fig. 4. A recent measurement<sup>10</sup> has shown the cross section for the reaction,  $P^{31}(N^{14}, \gamma)Ti^{45}$ , to be  $1 \mu b$  at a bombarding energy of 27 MeV. Since capture cross sections are extremely small and  $Cr^{49}$  is the compound nucleus formed from  $Cl^{35}$ , it is assumed to result from the reaction,  $Cl^{37}(N^{14}, 2n)Cr^{49}$ . The remainder of the investigated radioactive products,  $V^{47}$ ,  $Ti^{45}$ ,  $Sc^{44}$ ,  $Sc^{44m}$ ,

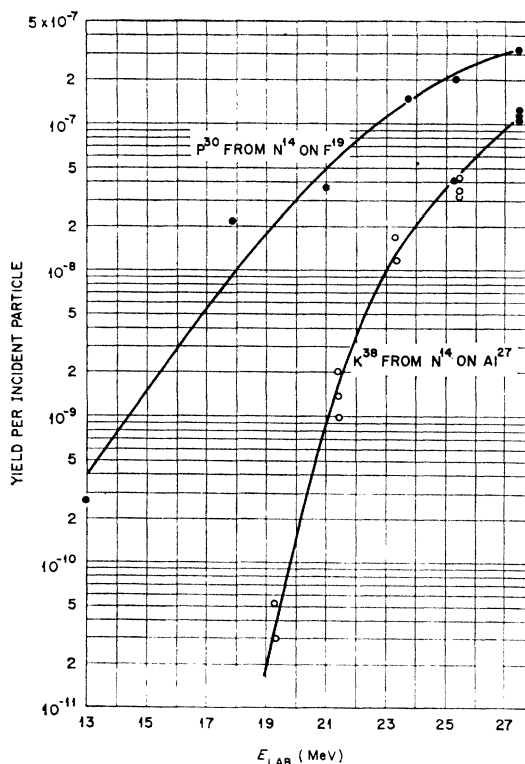


FIG. 3. Yields from reactions induced by  $N^{14}$  ions on aluminum and fluorine. For aluminum closed circles indicate the present data while open circles represent the data of Webb *et al.*

and  $Sc^{43}$ , were assumed to be produced primarily from  $Cl^{35}$ . Conceivably these reaction products could be made from  $Cl^{37}$  by the emission of two additional neutrons. However, in the process the  $Q$  values are decreased by approximately 19 MeV.

## Phosphorus

The yield of one reaction product,  $Sc^{43}$ , was studied with a phosphorus target. The yield curve is shown in Fig. 2; the calculated cross section is given in Table III. The isotope  $Sc^{43}$  is produced by a combination of the

<sup>10</sup> B. Linder and A. Zucker, Phys. Rev. **127**, 1280 (1962).

two reactions  $P^{31}(N^{14},pn)Sc^{43}$  and  $P^{31}(N^{14},2n)Ti^{43}$ . The nuclide  $Ti^{43}$  has a half-life of 0.6 sec and, therefore, by the time that counting was initiated it had decayed into  $Sc^{43}$ . An estimate of the  $2n$  contribution may be obtained from the chlorine data. There the ratio  $2n:2n+pn$  was measured to be  $\sim 0.1$ . This ratio would be expected to remain about the same for the  $P^{31}$  case since the  $Q$  values for the chlorine and phosphorus reactions are all similar.

### Silicon

In the bombardment of silicon, two products were identified:  $Cl^{34m}$  and  $K^{38}$ . The yield curves for these are shown in Fig. 2. The product  $K^{38}$  may be produced via the reactions:  $Si^{28}(N^{14},\alpha)K^{38}$ ;  $Si^{29}(N^{14},an)K^{38}$ ; and  $Si^{30}(N^{14},a2n)K^{38}$ . The natural abundances of  $Si^{28}$ ,  $Si^{29}$ , and  $Si^{30}$  are 92.2%, 4.7%, and 3.1%, respectively. On the basis of isotopic abundance, it might be argued that the reaction with  $Si^{28}$  need only be considered. However, reactions induced by 27.5-MeV  $N^{14}$  and proceeding by the emission of two particles are known to have much larger cross sections than reactions in which single

TABLE III. Measured cross sections.

Target	Product	Emitted particles	$\sigma$ at 26.5 MeV (mb)
$B^{11}$	$Ne^{23}$	$2p$	6.35
$Si^{28}$	$Cl^{34m}$	$2\alpha$	5.91
$Si^{28}$	$K^{38}$	$\alpha$	5.55 <sup>a</sup>
$Si^{29}$	$K^{38}$	$\alpha n$	108.9 <sup>a</sup>
$P^{31}$	$Sc^{43}$	$pn+2n$	57.43

<sup>a</sup> The cross section for the product  $K^{38}$  was calculated by assuming it was produced entirely from the isotope listed.

particles are emitted. Therefore, even if  $Si^{29}$  constitutes only 4.7% of silicon, a large portion of the detected  $K^{38}$  must have been made by the second reaction,  $Si^{29}(N^{14},an)K^{38}$ . The low abundance of  $Si^{30}$  (3.1%) and the fact that  $(N^{14},a2n)$  and  $(N^{14},\alpha)$  reactions have comparable cross sections<sup>7</sup> rules out the possibility that a large amount of  $K^{38}$  was made from  $Si^{30}$ . Two cross sections are listed in Table III for  $K^{38}$ , one for it to be produced exclusively from  $Si^{28}$  and the other for it to be made only from  $Si^{29}$ . Because of the ambiguity present in the case of  $K^{38}$ , the silicon cross section ratios could not be compared with the theoretical ones. The silicon reactions are, therefore, not considered any further.

For  $Cl^{34m}$  no similar ambiguity is present. At 27.5-MeV incident energy, the  $(N^{14},2\alpha)$  cross sections are known to be low.<sup>7,8</sup> The ejection of an extra one or two neutrons should lower the cross section further. This expectation coupled with the low abundances of  $Si^{29}$  and  $Si^{30}$  makes it virtually certain that  $Cl^{34m}$  is made essentially only from  $Si^{28}$  by the reaction  $Si^{28}(N^{14},2\alpha)Cl^{34m}$ . The cross section is listed in Table III.

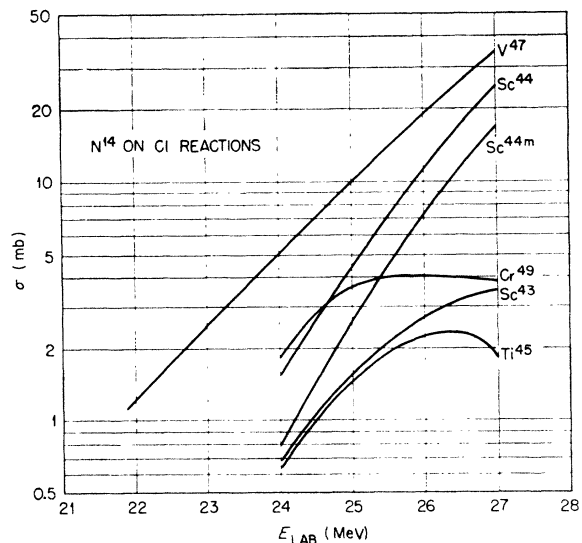


FIG. 4. Excitation functions for reactions induced by  $N^{14}$  ions on chlorine.

### Aluminum

The production of  $K^{38}$  from aluminum was studied. This isotope can result from two reactions,  $Al^{27}(N^{14},p2n)K^{38}$  and  $Al^{27}(N^{14},3n)Ca^{38}$ .  $Ca^{38}$  decays into  $K^{38}$  with a half-life of 0.7 sec. The results extend the earlier data of Webb, Reynolds, and Zucker,<sup>5</sup> whose maximum incident  $N^{14}$  energy was 25.5 MeV. The yield curve for the reaction is shown in Fig. 3; closed circles indicate the present data, while open circles show the experimental points obtained by Webb *et al.*<sup>5</sup> The agreement between the two sets of data is well within the experimental error despite the fact that the experimental methods used in the two studies were quite different. In the previous work the potassium fraction was

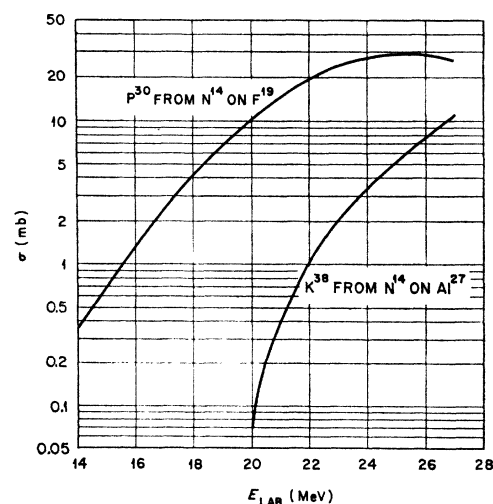


FIG. 5. Excitation functions for reactions induced by  $N^{14}$  ions on aluminum and fluorine.

chemically isolated and the purified sample beta counted under a shielded Geiger counter. Here,  $K^{88}$  was identified by the 7.7-min decay of its annihilation radiation, and no chemical separations were made. The excitation function for the reaction is shown in Fig. 5.

### Fluorine

The yield of  $P^{30}$  from fluorine was studied at  $N^{14}$  energies ranging from 13.0 to 27.5 MeV. The isotope can be produced from the two reactions  $F^{19}(N^{14}, p2n)P^{30}$  and  $F^{19}(N^{14}, 3n)S^{30}$ ; the half-life of  $S^{30}$  is 1.4 sec. The yield curve for the reaction is shown in Fig. 3, while the excitation function is displayed in Fig. 5.

### Boron-11

Boron enriched in  $B^{11}$  to 98.7% was bombarded with  $N^{14}$  and the reaction  $B^{11}(N^{14}, 2p)Ne^{23}$  was investigated. The yield curve is shown in Fig. 2; the cross section is given in Table III.

### Comparison with Theory

In the present investigation cross sections were measured for the production of four isotopes from the  $N^{14}$  bombardment of  $Cl^{35}$ , i.e.,  $V^{47}$ ,  $Ti^{45}$ ,  $Sc^{44}$ , and  $Sc^{48}$ . These experimental data for final isotopes resulting from one compound nucleus ( $Cr^{49}$ ) can be compared with the predictions of the statistical theory. The theory of the emission of particles from an excited compound nucleus is originally due to Weisskopf.<sup>11</sup> Recently in a series of papers, Dostrovsky *et al.*<sup>12</sup> have described a Monte Carlo calculation based upon this theory. An IBM 7090 program duplicating this approach has become available at this Laboratory.<sup>13</sup> This program was utilized to determine the applicability of the Monte Carlo calculations in their present form for the compound system  $N^{14}$  on  $Cl^{35}$ . No modifications were made to include the effect of nuclear clusters on the initial states of the cascades.

Two series of 100 case histories were run at  $N^{14}$  incident energies of 27 and 24 MeV to determine, as a function of the level density parameter  $a$ , the number of case histories ending in each final nuclide; the values of  $a$  ranged from 1 to 10. In this manner the value of  $a$  best fitting the data could be determined. It was found that the predicted ratios did not agree with the experimental ratios for any value of  $a$ . The best agreement was found, however, when  $a$  was equal to 1.70. The experimental cross-section ratios are compared in Table IV with two sets of theoretical ratios, one for  $a=1.70$  and the other for  $a=A/8$ , where  $A$  is the mass

TABLE IV.  $N^{14}$  on  $Cl^{35}$ , experimental and theoretical cross section ratios.<sup>a</sup>

$N^{14}$ energy (MeV)	Products	Experimental	Theoretical $a=1.70$	Theoretical $a=6.13$
27.0	$Sc^{44} (\alpha p)$	$1.18 \pm 0.28$	$0.26 \pm 0.01$	$0.085 \pm 0.009$
	$V^{47} (pn+2n)$			
	$Sc^{44} (\alpha p)$	$20.0 \pm 4.74$	$13.1 \pm 2.1$	b
	$Ti^{45} (a)$			
	$V^{47} (pn+2n)$	$17.0 \pm 4.03$	$49.6 \pm 7.7$	b
	$Ti^{45} (a)$			
	$Sc^{44} (\alpha p)$	$11.8 \pm 2.8$	$35.0 \pm 9.2$	$10.5 \pm 3.5$
	$Sc^{48} (\alpha pn)$			
	$V^{47} (pn+2n)$	$10.0 \pm 2.4$	$132.3 \pm 33.6$	$123.5 \pm 39.3$
	$Sc^{48} (\alpha pn)$			
24.0	$Sc^{44} (\alpha p)$	$0.43 \pm 0.10$	$0.19 \pm 0.01$	$0.07 \pm 0.006$
	$V^{47} (pn+2n)$			
	$Sc^{44} (\alpha p)$	$3.75 \pm 0.89$	$6.07 \pm 0.78$	$13.5 \pm 4.4$
	$Ti^{45} (a)$			
	$V^{47} (pn+2n)$	$8.67 \pm 2.06$	$31.8 \pm 0.78$	$192.0 \pm 60.9$
	$Ti^{45} (a)$			
	$Sc^{44} (\alpha p)$	$3.46 \pm 0.82$	b	b
	$Sc^{48} (\alpha pn)$			
	$V^{47} (pn+2n)$	$8.00 \pm 1.89$	b	b
	$Sc^{48} (\alpha pn)$			

<sup>a</sup> Theoretical ratios obtained from 1000 case histories.

<sup>b</sup> No tabular entry indicated failure of calculation to predict the final nuclide in the denominator.

number of the compound nucleus. For this comparison, 1000 case histories were run for each set of  $a$  and  $N^{14}$  energy. It is seen that the  $a=1.70$  sets do agree slightly better with experiment. Ratios calculated for values of  $a$  between 1.70 and  $A/8$  gave results intermediate between the tabulated values. For  $a < 1.70$  the fit was also worse than for  $a=1.70$ .

The reason for the poor agreement and the necessity for a low value of  $a$  can be seen from Fig. 6. Here are plotted the number of emitted neutrons, protons, deuterons, and alphas versus  $a$  for an  $N^{14}$  energy of 27 MeV.<sup>14</sup> The Monte Carlo calculations predict very few emitted alphas in comparison to neutrons and protons. The experimental data, on the other hand, clearly show that alpha emission competes successfully with neutron and proton emission. Thus the dearth of predicted alpha emission is responsible for the lack of agreement with experiment. In addition, it is seen that the alpha curve in Fig. 6 peaks for  $a \sim 1.70$ . This is the reason why one is forced to select a low value to obtain the best fit with experiment.

<sup>11</sup> V. F. Weisskopf, Phys. Rev. **52**, 295 (1937).

<sup>12</sup> I. Dostrovsky, Z. Fraenkel, and G. Friedlander, Phys. Rev. **116**, 683 (1959); I. Dostrovsky, Z. Fraenkel, and L. Winsberg, *ibid.* **118**, 781 (1960); I. Dostrovsky, Z. Fraenkel, and P. Rabinowitz, *ibid.* **118**, 791 (1960).

<sup>13</sup> The authors wish to express their appreciation to L. Dresner for making this 7090 program available to them.

<sup>14</sup> The compound nucleus,  $Cr^{49}$ , is neutron deficient and thus accounts for the preponderance of the emission of protons over that of neutrons. A similar survey on  $N^{14}+Cl^{37}$ , (the compound nucleus,  $Cr^{51}$ , is only one neutron away from the beta-stability line), at the same incident energy, almost exactly interchanged the number of emitted protons and neutrons but left the deuteron and alpha curves unchanged.

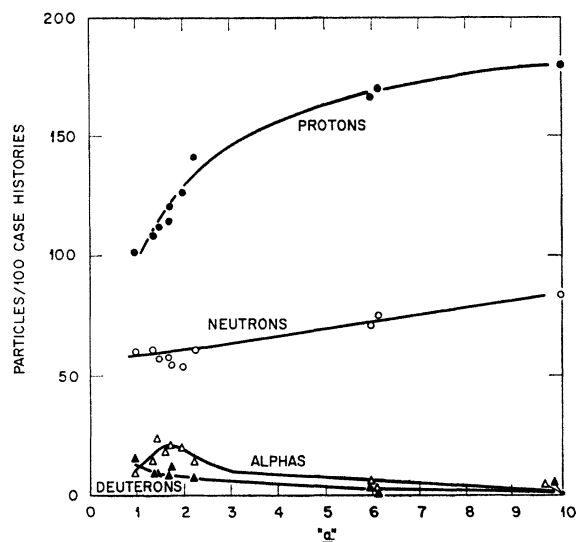


FIG. 6. Number of particles emitted from the compound system  $N^{14}+Cl^{38}$  at an incident energy of 27.5 MeV plotted as a function of the level density parameter  $a$ . The number of particles was calculated per 100 case histories with a Monte Carlo evaporation code. Results of the calculation are shown only for neutrons, protons, deuterons, and alpha particles. The curves are drawn only to help observe the variation of the number of emitted particles with  $a$ .

The value of  $a$  most commonly cited in the literature, excluding the regions near magic numbers, is  $a \sim A/10$ . Several possible explanations exist for the appearance of a small value of the level density parameter and the poor agreement between theoretical and experimental cross-section ratios. These include the absence of an  $E^{-2}$  term in the level density expression, and the fact that angular momentum effects and  $\gamma$ -ray de-excitations are not considered.

Another possibility for the discrepancy between the theoretical and experimental ratios is the method of calculating the probability of emission for the various particles. The probability that an excited nucleus will emit a particle  $X$  is proportional to  $\sigma_{ex}$ , the formation cross section. Inverse cross sections for neutrons, protons, and alpha particles were calculated from the analytical expression chosen by Dostrovsky to approximate square well potential cross sections. These were compared to the corresponding cross sections calculated from optical-model transmission coefficients. The optical model code used was that written by Bassel and Drisko,<sup>15</sup> while the parameters were based on the results

<sup>15</sup> The authors wish to thank R. H. Bassel and R. M. Drisko for making available their IBM-7090 code "Leonora" and for

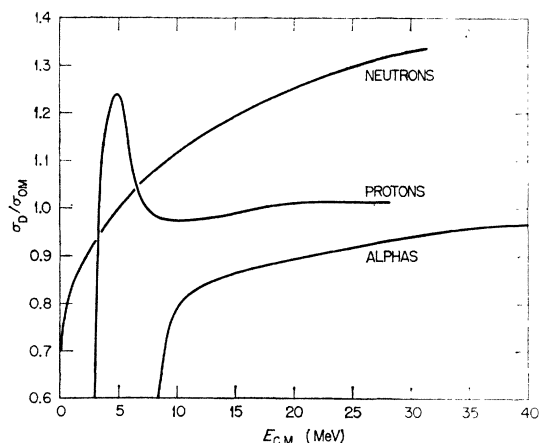


FIG. 7. Ratios of inverse cross sections for protons, neutrons, and alpha particles;  $\sigma_D$  was obtained from expression in reference 12, while  $\sigma_{OM}$  was determined from optical-model transmission coefficients.

of Bassel, Satchler, Drisko, and Rost.<sup>16</sup> Figure 7 is a plot of the ratio of the inverse cross sections obtained by applying the analytical form of Dostrovsky *et al.* to the optical-model cross sections as a function of the center-of-mass energy. The curves were calculated for  $n+Cr^{48}$ ,  $p+V^{48}$ , and  $\alpha+Ti^{46}$ . Except for the region at the Coulomb barrier, the proton cross sections agree very well. The Dostrovsky neutron cross section is low at small energies, then crosses the optical model prediction at  $\sim 5$  MeV, and increases to 30% above the optical model at high energies. The alpha curve, on the other hand, starts out low and asymptotically approaches the ratio of 1. The combination of effects depresses alpha-particle emission probability by approximately 20%. While this does partially explain the disagreement between experiment and theory for alpha-out reactions, the over-all effect is insufficient to account for the discrepancy.

#### ACKNOWLEDGMENTS

The authors wish to thank R. H. Bassel, M. L. Halbert, and A. Zucker for their helpful comments. They also wish to thank T. H. Handley who performed the chemical separations and G. A. Palmer who plotted most of the  $\gamma$ -ray spectra.

their assistance in the calculation of the optical model inverse cross sections.

<sup>16</sup> R. H. Bassel, G. R. Satchler, R. M. Drisko, and E. Rost, *Phys. Rev.* **128**, 2693 (1962).